Summer Sea Surface Temperature Conditions in the North Atlantic and Their Impact upon the Atmospheric Circulation in Early Winter

CHRISTOPHE CASSOU

Climate Global Dynamics Division, NCAR, Boulder, Colorado, and Climate Modelling and Global Change Team, SUC, CERFACS, Toulouse, France

CLARA DESER

Climate Global Dynamics Division, NCAR, Boulder, Colorado

LAURENT TERRAY

Climate Modelling and Global Change Team, SUC, CERFACS, Toulouse, France

JAMES W. HURRELL

Climate Global Dynamics Division, NCAR, Boulder, Colorado

MARIE DRÉVILLON

Climate Modelling and Global Change Team, SUC, CERFACS, Toulouse, France

(Manuscript received 26 February 2003, in final form 3 February 2004)

ABSTRACT

The origin of the so-called summer North Atlantic ''Horseshoe'' (HS) sea surface temperature (SST) mode of variability, which is statistically linked to the next winter's North Atlantic Oscillation (NAO), is investigated from data and experiments with the CCM3 atmospheric general circulation model (AGCM). Lagged observational analyses reveal a linkage between HS and anomalous rainfall in the vicinity of the Atlantic intertropical convergence zone. Prescribing the observed anomalous convection in the model generates forced atmospheric Rossby waves that propagate into the North Atlantic sector. The accompanying perturbations in the surface turbulent and radiative fluxes are consistent with forcing the SST anomalies associated with HS. It is suggested that HS can therefore be interpreted as the remote footprint of tropical atmospheric changes.

The ARPEGE AGCM is then used to test if the persistence of HS SST anomalies from summer to late fall can feed back to the atmosphere and have an impact on the next winter's North Atlantic variability. Observed HS SST patterns are imposed in the model from August to November. They generate a weak but coherent early winter response projecting onto the NAO and therefore reproduce the observed HS–NAO relationship obtained from lagged statistics. Changes in the simulated upper-level jet are associated with the anomalous HS meridional SST gradient and interact with synoptic eddy activity from October onward. The strength and position of the transients as a function of seasons are hypothesized to be of central importance to explain the nature, timing, and sign of the model response.

In summary, the present study emphasizes the importance of summer oceanic and atmospheric conditions in both the Tropics and extratropics, and their persistence into early winter for explaining part of the NAO's low-frequency variability.

1. Introduction

Over the last couple of years, interest in the low-frequency variability of North Atlantic climate has increased markedly (e.g., Marshall et al. 2001; Stephenson et al. 2003). In particular, attention has been focused on the North Atlantic Oscillation (NAO), described as the most prominent and recurrent pattern of atmospheric variability (Wallace and Gutzler 1981). Important ecological, economical, and societal impacts that the NAO exerts on the entire Northern Hemisphere have been documented and questions have been raised about its potential predictability (Hurrell 2003). Although the NAO mainly arises from internal atmospheric interac-

---

Corresponding author address: Dr. Christophe Cassou, CERFACS-SUC (URA 1875), Climate Modelling and Global Change Team, 42 Ave. Gustave Coriolis, 31057 Toulouse, France.
E-mail: cassou@cerfacs.fr

tions, external forcings such as sea surface temperature (SST) anomalies or increasing greenhouse gases, etc. might affect the occurrence and/or the persistence of its phase. Their influence could be important for understanding both amplitude and long-term evolution of the NAO in the context of climate change or climate predictability.

On one hand, the impact of atmospheric circulation anomalies upon extratropical/subtropical oceans has been demonstrated in numerous studies (see, e.g., Battisti et al. 1995). Anomalous turbulent heat fluxes, buoyancy-driven entrainment and Ekman advection are the main processes whereby the atmosphere imprints large-scale SST anomalies. In such a scenario, the extratropical atmosphere primarily leads the midlatitude ocean variability by a month or so, as examined for instance in Deser and Timlin (1997) or Frankignoul et al. (1998). The low frequency oceanic anomalies are considered as the *passive* temporal integration of the atmospheric stochastic forcing (Frankignoul and Hasselmann 1977).

On the other hand, although the atmospheric fluctuations are undoubtly the dominant driver of the upper-ocean anomalies, the role of the ocean has been suggested to explain the reddening of the atmospheric fluctuations from seasonal to decadal time scales. For instance, Rodwell et al. (1999) and Mehta et al. (2000) using atmospheric global circulation models (AGCMs) forced by historical global SST estimations have been able to reproduce some of the low-frequency variability of the winter NAO during the last 50 years. The dominant influence of the tropical/subtropical Atlantic oceanic basin has been inferred in some studies (e.g., Sutton et al. 2001). Terray and Cassou (2002) diagnose from model simulations that anomalous SSTs there alter the local atmospheric Hadley cell over the western tropical basin, providing an anomalous source of Rossby waves (Sardeshmukh and Hoskins 1988) extending northeastward from the Caribbean toward Europe. The phase of the NAO is ultimately affected by this teleconnection mechanism as described in Peng et al. (2003), Drévillon et al. (2003), and Cassou et al. (2004). Hoerling et al. (2001) argued that the whole Tropics, not just the Atlantic domain, must also be considered. In particular, the role of the Indian Ocean has been suggested by Sutton and Hodson (2003) and Hurrell et al. (2004).

North Atlantic midlatitude SST anomalies may also have a nonnegligible influence on the variability of the NAO. The dominant mechanisms are discussed in Peng and Whitaker (1999) and Peng and Robinson (2001). They emphasize the role of synoptic storm activity and associated eddy–mean flow interaction that can be perturbed by the existence of anomalous meridional SST gradients along the subpolar–subtropical gyre front. Extratropical oceanic anomalies may also contribute to the reddening of the NAO spectrum in the interannual band through the reemergence mechanism in which upper-ocean temperature anomalies created over a deep mixed layer in winter are preserved within the highly stratified summer thermocline (Deser et al. 2003). As they reappear at the surface at the next late fall or early winter by reentrainment (de Coëtlogon and Frankignoul 2003), they may have a feedback impact upon the overlying atmosphere. However, conclusions about extratropical SST forcing upon the North Atlantic atmosphere are very model dependent [see Robinson (2000) or Kushnir et al. (2002) for a review] and should be taken with caution. The models' different sensitivities appear to be due to a different representation of the simulated climatological flow and internal atmospheric modes of variability.

At monthly to seasonal time scales, lagged relationships between the early wintertime North Atlantic atmosphere and the previous summer–fall oceanic conditions have been documented by Czaja and Frankignoul (1999, 2002) and Drévillon et al. (2001). Using singular value decomposition (SVD), a statistical link is extracted between the so-called summer North Atlantic ''Horseshoe'' (HS) SST pattern and the NAO, as illustrated in Fig. 1 using data from the National Centers for Environmental Prediction–National Center for Atmospheric Research (NCEP–NCAR) reanalysis (Kalnay et al. 1996). The negative phase of the NAO (Fig. 1a) in early winter [October–December (OND) mean] is characterized by a slackening of the Icelandic low and the Azores high, and is associated with late summer [August–September (AS) mean] negative SST anomalies located southeast of Newfoundland and extending westward slightly along the Gulf Stream path, surrounded by positive anomalies on the eastern side of the Atlantic (Fig. 1b). Maximum warming occurs off the northern African coast and from Britain to the southern tip of Greenland. The HS mode is dominated by interannual fluctuations with a tendency toward dominant positive phases in the 1950s and 1960s and more recurrent negative phase from the early 1970s to the early 1990s (Fig. 1c). Watanabe and Kimoto (2000) and Drévillon et al. (2001, 2003), from data and model experiments respectively, speculate on physical processes responsible for the statistical lagged properties shown in Fig. 1, but the nature of the summer ocean influence on the next winter NAO is still unclear.

The main goal of this paper is to go beyond statistical analyses and to suggest a physical explanation for the existence of the summer HS pattern and a hypothesis for the lagged relationship between that SST pattern and the following winter atmospheric conditions. The observational results are used to motivate several model experiments to test these ideas. The paper is organized as follows. A combined observation–model analysis is presented in section 2 to illustrate the relationship between anomalous summer atmospheric conditions over the Atlantic and the oceanic HS mode. Interpretations about the origin of the HS are discussed. The lagged influence exerted by the HS on the North Atlantic wintertime atmosphere is then examined in section 3. The observed HS monthly evolution is prescribed from late

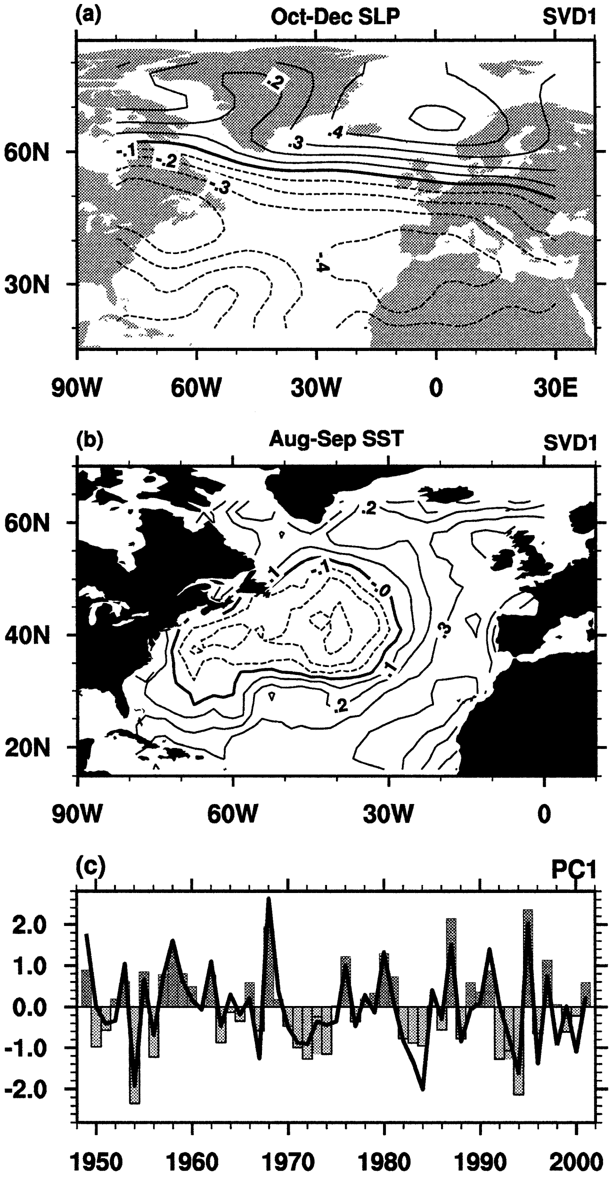

FIG. 1. First singular value decomposition modes calculated between (a) OND SLP (hPa) and (b) AS SST (°C) computed from NCEP–NCAR over the 1949–2001 period. The covariance between the two modes is equal to 63.9%. Contour intervals are respectively 0.1 hPa and 0.1°C. (c) Normalized time series related to the AS SST (bars) and OND SLP (solid line) leading SVD mode. The correlation between the two PC time series reaches 0.72 (significant at 99%).

summer to early winter in a model to investigate its impacts on the North Atlantic atmospheric dynamics. A synthesis and discussion are provided in section 4.

2. Origin of the late summer North Atlantic "Horseshoe" SST mode

a. Motivation: Observational results

The origin of the late summer HS mode that exhibits the strongest covariability with the next winter NAO (Fig. 1) is investigated first from observations. To clearly identify the role of the atmosphere in the origin of the ocean anomalous pattern, June–July (JJ) averaged atmospheric fields have been regressed onto the AS averaged SST SVD principal component (PC) time series. All atmospheric fields have been quadratically detrended prior to the regression.

There is some evidence that the extratropical HS mode is forced in part by atmospheric circulation anomalies through modifications of the surface turbulent and radiative fluxes. The lagged regression of the total surface heat flux estimated from the Comprehensive Ocean–Atmosphere Data Set (COADS; Woodruff et al. 1998) following the Cayan (1992) formulation matches the spatial pattern of the HS SST anomalies fairly well, with the atmosphere tending to warm the subtropical and eastern Atlantic and to cool the western basin (Fig. 2a).

The turbulent flux contribution can be mainly understood in terms of near-surface wind changes (Fig. 2b). The anomalous cyclonic circulation located off Newfoundland induces anomalous northerlies over the western part of the basin, slackened westerlies at higher latitudes especially in the Labrador and Irminger Seas, and reduced trade winds within the subtropics in the central Atlantic. Cold air is advected from the north on the western side of the basin, cooling the ocean mixed layer, while decreased winds within the band 50°–65°N reduce the turbulent heat flux, warming the mixed layer. Besides, Ekman pumping due to the anomalous cyclonic circulation over the basin may contribute to cooling down the ocean surface off Newfoundland (not shown). Advection is also expected to explain part of the anomalies along the Gulf Stream path where local wind anomalies are not clearly related to surface oceanic conditions.

The trade winds are not significantly modified in the eastern subtropical basin where the maximum warming occurs. Over this specific region, the radiative balance at the surface might have a complementary or even greater role. Decreased cloudiness is observed on the eastern side of the Atlantic basin especially within the subtropical band and off Europe (Fig. 2c), consistent with the higher SSTs. Reduced low-level clouds that are dominant over this area diminish the so-called albedo feedback and tend to warm up the surface ocean. Increased cloudiness over most of the anomalous SST cold core reinforces the cooling of the ocean mixed layer due to enhanced turbulent heat loss. Although less significant and less large scale, the NCEP–NCAR surface shortwave flux anomalies match the COADS cloudiness results. The cloud pattern is persistent until fall (not shown) and may contribute to maintain the ocean surface anomalies. This is particularly true above the subtropical SST lobe. The western tropical Atlantic basin (west of 60°W) is characterized by increased cloudiness over positive SST anomalies. Low-level stratiform clouds are fairly sparse over this area dominated by

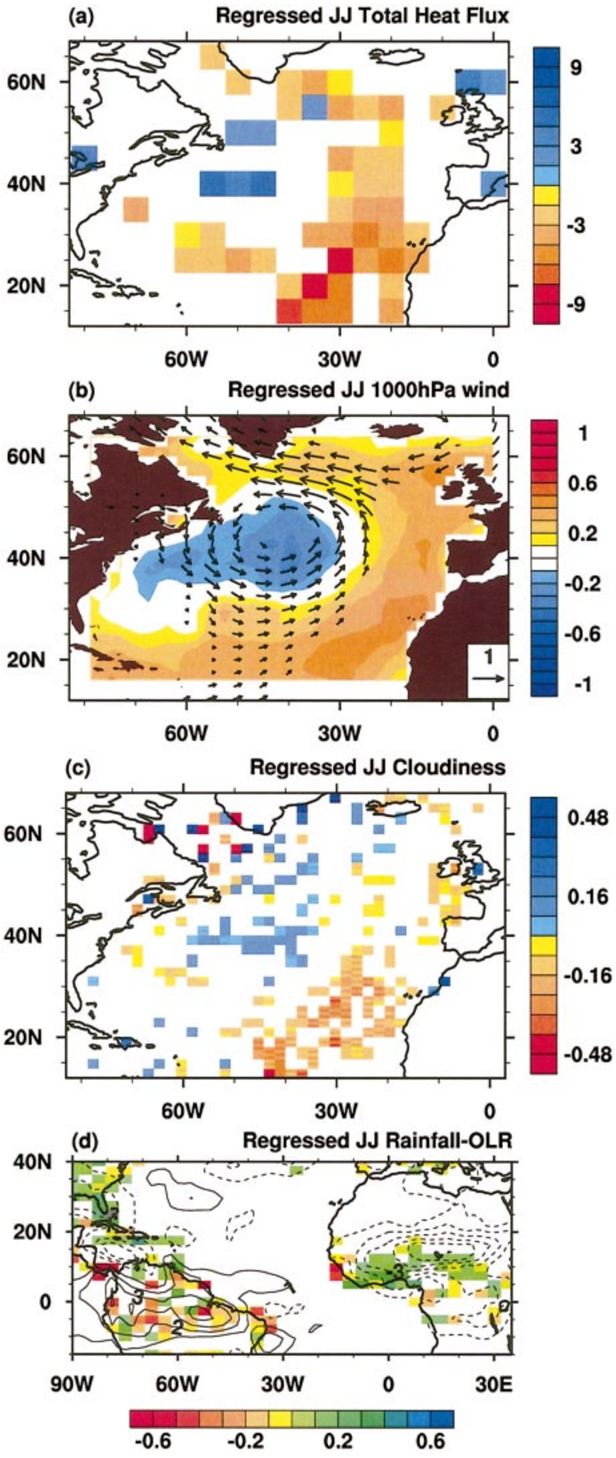

FIG. 2. Two-month lead (JJ) regression onto the AS SST PC of (a) total surface heat flux (W m^{-2}) from COADS and (b) 1000-hPa NCEP–NCAR wind superimposed on the SVD SST mode itself. Contour intervals are 0.1°C. (c) Cloudiness (octas) from COADS and (d) OLR (W m^{-2}) (contour) from NCEP–NCAR and rainfall station-based data (mm day^{-1}) from Hulme and New (1997) (contour interval is 1 W m^{-2} for OLR and positive values are indicative of decrease convection). Only points satisfying the 90% level confidence are plotted for all the datasets.

convection, and this pattern suggests some strengthening of the convective activity.

We investigate this signal further using NCEP–NCAR outgoing longwave radiation (OLR) as a proxy for deep convection in the Tropics. As accurate measurements have been only available from satellites since the late 1970s, station-based precipitation data (Hulme and New 1997) are used to further confirm the robustness of our finding from OLR. The HS mode is associated with early summer enhanced convective activity (decreased OLR) over Africa and over the Caribbean Sea extending northwestward toward Florida (Fig. 2d). Such an increase of convection within the band 10°–20°N, indicative of a slight northward shift and intensification of the intertropical convergence zone (ITCZ), contrasts with mostly dry conditions over the Amazonian basin (increased OLR). The precipitation station data confirm the OLR signal over land (Fig. 2d) and are consistent with increased cloudiness over the Caribbean diagnosed independently from COADS. The anomalous rainfall pattern shown in Fig. 2d is similar to that documented by Giannini et al. (2003) at interdecadal time scale and by Sutton et al. (2000) and Okumura et al. (2001) at interannual time scales. As shown by Fontaine et al. (1999), when the SST anomalies are positive in the northern tropical Atlantic, the local Hadley circulation is altered with increased low-level convergence from Gulf of Guinea to the Sahel bringing more moisture over land consistent with enhanced convection. By contrast, mostly dry conditions dominate along the equator over sea and over the South American continent.

b. CCM3 model experiments

We have shown from observations that the late summer North Atlantic SST anomalies associated with the HS mode are likely a lagged local response to the extratropical underlying atmospheric changes. We have also shown that HS is preceeded by anomalous tropical atmospheric anomalies. To explore the extent to which tropical Atlantic rainfall changes can affect the midlatitude atmosphere in summer and how these are linked to HS, two experiments are conducted with the third version of the NCAR Community Climate Model (CCM3), which has a T42 triangular horizontal resolution and 18 vertical levels. A complete description of the physical and numerical methods used in CCM3 is provided in Kiehl et al. (1996) and model validation is given in Hurrell et al. (1998). The summer ITCZ intensity is artificially perturbed in the model based upon the observed anomalous convection pattern associated with HS (Fig. 2d). Two idealized heat sources have been specified, one centered over the Caribbean Sea and one over the Sahel region (rectangles in Fig. 3a). The vertical distribution of the heating perturbation (Fig. 3b) reaches a maximum intensity at 500 hPa and is equal to +2°C day^{-1}, which roughly corresponds to twice the maximum observed changes estimated from the

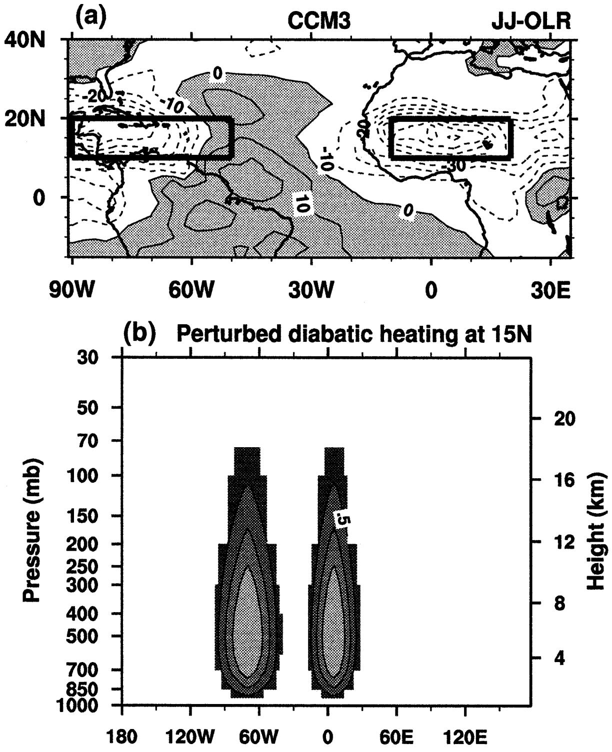

FIG. 3. (a) The JJ 2-month-averaged difference for OLR (W m^{-2}) between anomalous prescribed diabatic "heating" and diabatic "cooling" CCM3 experiments. Contour interval is 10 W m^{-2} and shading stands for positive anomalies. Convention is negative OLR for increased convection. The thick solid boxes represent the geographical domains where the anomalous diabatic heating/cooling is prescribed in CCM3. (b) Anomalous diabatic heating vertical profile (°C day^{-1}) for a section at 15°N as a function of longitude and prescribed in CCM3. Contour interval is 0.5°C day^{-1}.

NCEP–NCAR reanalyses. A twin experiment with a prescribed -2°C day^{-1} is also carried out and the model is integrated for 10 summers in both cases. The reader is invited to refer to Branstator and Haupt (1998) for a complete description of the experimental setup. The choice for the strong magnitude of the perturbation applied in the model is dictated by our attempt to better extract the tropical impact onto the midlatitude dynamics within the constraint of limited computing resources. In the following, we focus our explanation on the linear [(heating $-$ cooling)/2] response.

As expected, the model shows enhanced convective activity collocated with the prescribed anomalous diabatic heating (Fig. 3a). Maximum OLR anomalies reach about -60 W m^{-2} centered over the Sahel and Caribbean. Diminished convection appears over the South American continent and the western equatorial Atlantic, reminiscent of the observations. Thus, the diminished convection may be interpreted as a remote response to the increased convection along the ITCZ in the model. We have also verified that specifying a negative heat source over Amazonia in the model leads to enhanced convection over the Caribbean and also to a lesser extent over the Sahel (not shown). This suggests that the full heating distribution in the whole tropical Atlantic may, in fact, play a role. Very similar conclusions are obtained from the upper-tropospheric convergence field (not shown).

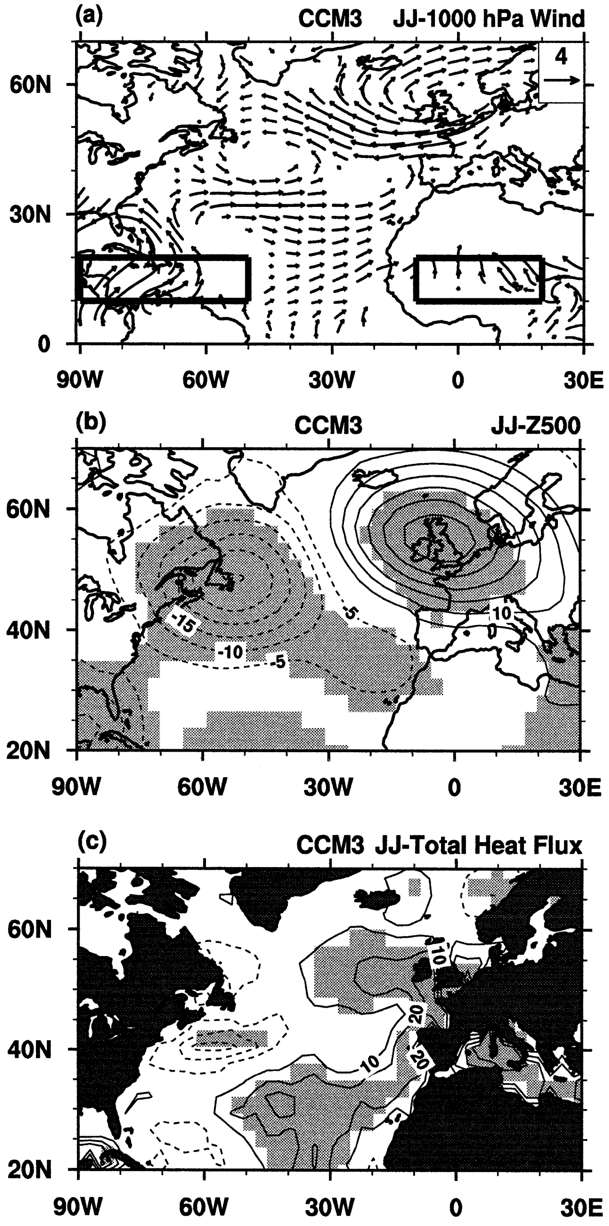

FIG. 4. As in Fig. 3a, but for CCM3 (a) wind at 1000 hPa, (b) geopotential height at 500 hPa (m) and (c) total heat flux (W m^{-2}). Contour intervals are 5 m and 10 W m^{-2}. Shaded areas exceed the 95% significance limit using *T* statistics.

The simulated low-level wind response to the heat sources is shown in Fig. 4a. Weakened trade winds dominate the subtropical North Atlantic basin, consistent with observations. Similarities can be also found between the modeled and observed surface wind changes at midlatitudes. Despite a slight westward and northward shift, the model is able to reproduce the cyclonic atmospheric circulation off Newfoundland in association with a stronger Atlantic ITCZ. The perturbed atmospheric circulation is reminiscent of a Rossby wave train pattern originating from the Gulf of Mexico and extending northeastward toward Scandinavia. Although such a mechanism is more active in winter–spring (Webster 1982), it seems to be at work also in summer in the model. It clearly dominates the remote midlatitude atmospheric changes as displayed in Fig. 4b for the 500-hPa geopotential height (hereafter *Z*500). Minimum *Z*500 is located around Newfoundland and slightly west of the low-level cyclonic conditions while high pressure over Britain is consistent with the surface anticyclone. Note that the latter is less evident in the observations (Fig. 2b). The overestimation of the Rossby wave extension simulated in CCM3 might be attributed to the higher intensity of the perturbation prescribed in the Tropics compared to observations or to the model oversensitivity for that particular season due to mean state biases. To measure the importance of the remote signal, we note that the signal-to-noise ratio comparing forced variability (model response in sensitivity experiments) and internal variability (estimated from a control simulation of CCM3) is close to 1 off Newfoundland and drops to 0.6 over the United Kingdom.

To further confirm the teleconnection hypothesis and its origin, complementary simulations have been carried out by selecting only one of the two anomalous diabatic heating sources, thereby isolating the Sahel versus Caribbean impacts. Similarly to the previous experiments, the model is integrated for 10 summers and for the ‘‘heating’’ and the ‘‘cooling’’ cases. The Rossby-wave type anomalous circulation completely disappears in the Sahel-only experiment while a clear cyclonic circulation centered off the North African coast (30°N, 20°W) dominates (not shown). In that case, the slackening of the Atlantic trade winds is more pronounced since the low-level convergence to the Caribbean has been removed. By contrast, Caribbean-only experiments (not shown) reveal a clear Rossby wave train while the trade winds are reinforced in the western tropical basin but not affected in the eastern basin. This result is consistent with the fact that the western convection core is bordered on its northern side by climatological upper-level westerlies, whereas the African core is capped by easterlies, precluding any meridional propagation of tropical forced Rossby waves (Hoskins and Pierce 1983). Based on these model results, we suggest that the observed Atlantic wind pattern associated with the HS in summer can be viewed as a remote response to changes in tropical convection over both the Sahel and Caribbean regions, with the trade winds responding to both heat sources and the extratropical winds responding mainly to the Caribbean one.

Total surface heat flux anomalies over the subtropical/North Atlantic basin in the CCM3 experiments represent the local atmospheric forcing of the ocean mixed layer (Fig. 4c). The heat flux anomalies are consistent with anomalous low-level wind conditions and bear a strong resemblance to the observed pattern (Fig. 2a). Weaker trade winds are associated with diminished turbulent heat flux out of the ocean east of 50°W, which tends to warm up the subtropical North Atlantic. A secondary core centered around 50°N off Europe corresponds to the midlatitude slackening of the mean westerlies and similarly tends to warm up the northeast Atlantic. By contrast, the western side of the basin north of 20°N is dominated by enhanced evaporation and northerly winds that tend to cool down the surface ocean, although signals are rather weak and mostly confined south of Newfoundland close to the Gulf Stream. Decomposing the total heat flux into radiative and turbulent components (not shown) reveals that the latter dominates in the model except off the Iberian penisula where the simulated warming tendency appears to be limited to the coast (Fig. 4c) compared to observations (Fig. 2a). This confinement can be attributed to an overestimation of enhanced cloudiness in the model over this area (the CCM3 cloud response to the perturbed ITCZ is maximum to the east of the anomalous cyclonic circulation while in reality these are collocated, Fig. 2c). Except over this specific area, changes in radiation balance due to cloud cover are weak in the model and are suspected to be underestimated. This could be explained by the absence of local ocean feedback to the atmosphere due to the experimental configuration. In reality, local SST anomalies have been shown within the subtropics to locally affect the stability of the atmospheric column and thus amplify and/or maintain the anomalous cloud pattern (Norris et al. 1998). The weakness of the cloud impact could also be explained by the underestimation of low-level cloud amount in CCM3. Additional experiments using a newer version of CCM3 coupled to a complex ocean mixed layer model (Alexander et al. 2002) are currently in progress to examine the SST response to tropical diabatic heating anomalies.

3. Summer SST forcing of the NAO in early winter

a. Experimental setup

The speculated feedback of SST anomalies associated with the HS mode onto the early winter atmosphere over the North Atlantic–European sector is now examined through two 30-member ensemble integrations, each 9 months long (July–March), using the Action de Recherche Petite Echelle Grand Echelle (ARPEGE) model jointly developed by Météo-France and European Centre of Medium-Range Weather Forecasts (Déqué et al. 1994). The present climate version of ARPEGE uses a T63 triangular horizontal truncation. Diabatic fluxes and nonlinear terms are calculated on a gaussian grid of about 2.8° latitude × 2.8° longitude. The vertical is discretized over 31 levels (20 levels in the troposphere)

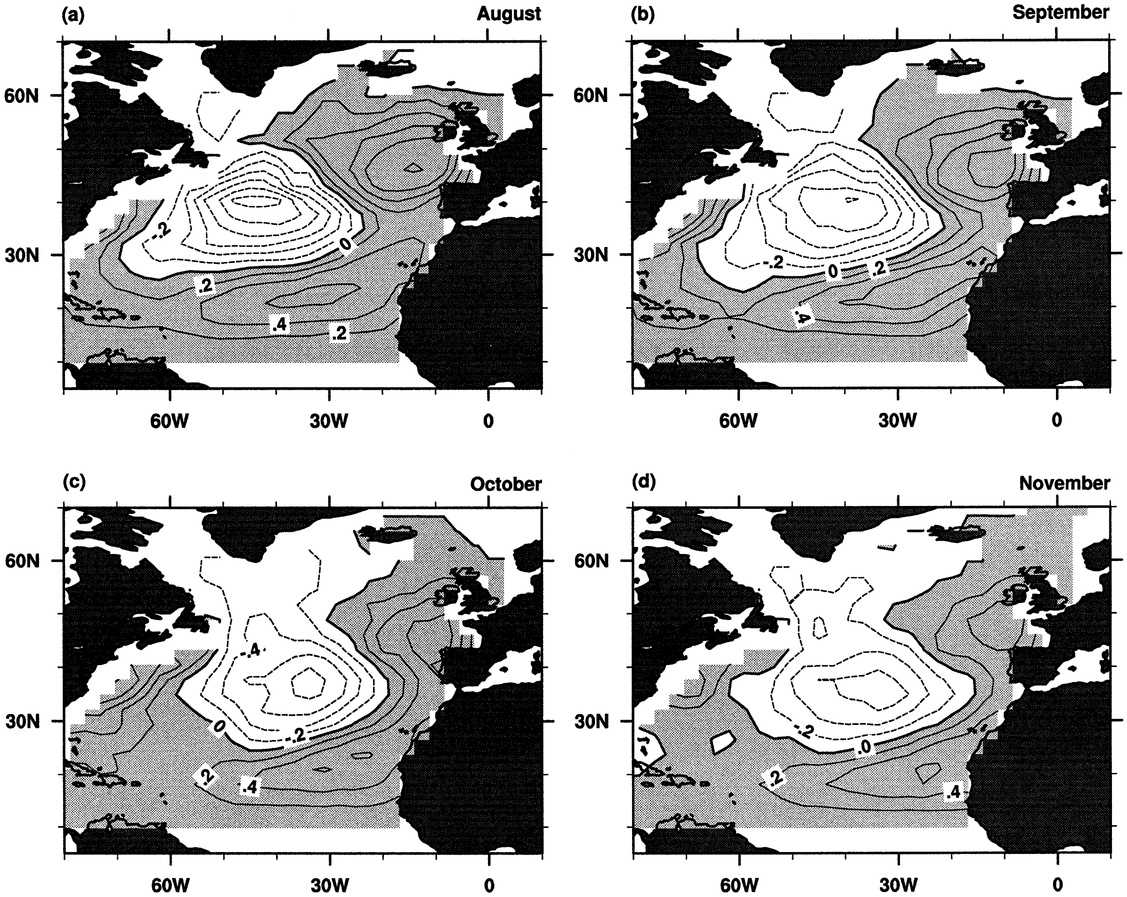

FIG. 5. Anomalous SST patterns (°C) added to (subtracted from) ARPEGE boundary conditions from (a) Aug to (d) Nov for the HS+ (HS−) experiment. Contour interval is 0.2°C and shading stands for positive anomalies.

using a progressive vertical hybrid coordinate extending from the ground up to about 34 km (7.35 hPa). Further details about the model physics package and about the validation of the simulated intraseasonal and interannual variability can be found in Doblas-Reyes et al. (1998, 2001) and in Cassou and Terray (2001).

The HS-type SST anomalies are either added to (hereafter HS+ experiment) or subtracted from (HS−) the model boundary conditions from 15 July to 15 December (Fig. 5), while late December to March oceanic conditions remain unperturbed and fixed to the seasonal climatology. The monthly anomalous SST patterns have been obtained by regression of monthly SST data upon the PC time series of the leading SVD mode shown in Fig. 1c. The intensity of the SST anomalies imposed in the model is given by the strongest value of the PC time series over the analyzed 52-yr period. For HS+, maximum cooling off Newfoundland reaches −1.2°C in August whereas subtropical values are slightly above +0.6°C off the northwest African coast. Maximum warming peaks at about +1°C off western Europe. The opposite is taken for HS−.

As described in Drévillon et al. (2001), the HS oceanic anomalies are fairly persistent from summer to early winter (the correlation between August and November PC time series calculated from empirical orthogonal function decomposition of the consecutive July–August–September–October–November normalized months and capturing HS is equal to 0.44). Consistent with their study, the extratropical lobes prescribed in our case exhibit a slow decay in amplitude with time (about 50% diminution from August to November), while a slight eastward propagation of the midlatitude SST core is noticeable. Compared to the extratropics, the subtropical oceanic anomalies are more persistent both in amplitude and space. The rate of decay of the tropical/subtropical SST anomalies are roughly consistent with the stochastic climate model (Frankignoul and Hasselmann 1977). In the following, we examine the linear $[(\langle \mathrm{HS}+\rangle - \langle \mathrm{HS}-\rangle)/2]$ component of model response (angle brackets standing for ensemble mean).

b. ARPEGE atmospheric response to HS SST anomalies

Zonal wind anomalies at 200 hPa (U200), Z500, and geopotential height anomalies at 1000 hPa (Z1000) are presented for the OND average for ARPEGE (Figs.

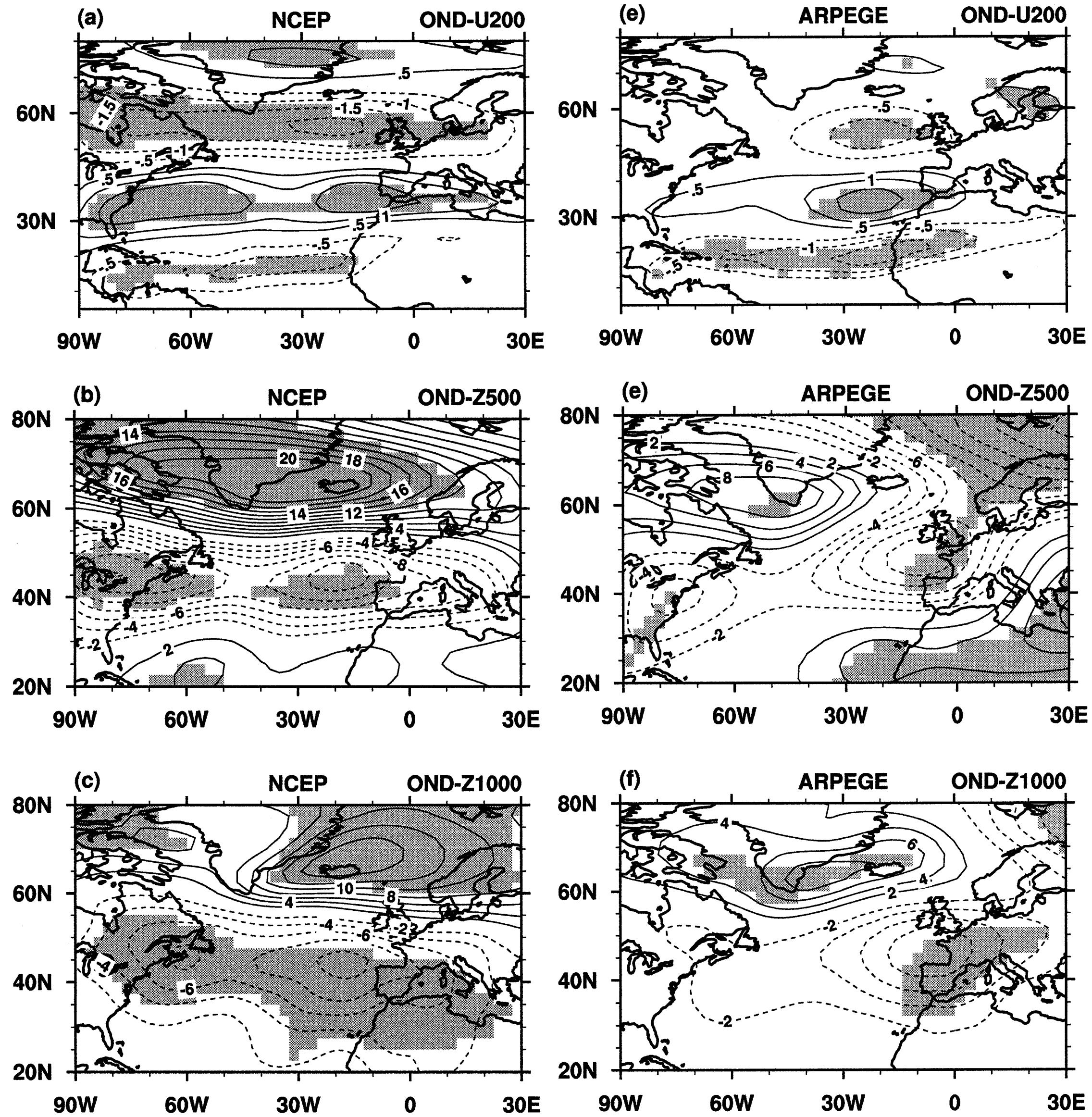

FIG. 6. Regression of NCEP–NCAR OND zonal wind at (a) 200 hPa (U200) (m s^{-1}), (b) geopotential height at 500 hPa (Z500) (m), and (c) at 1000 hPa (Z1000) (m), onto AS SST time series obtained from SVD. Linear ARPEGE response in OND for (d) U200, (e) Z500, and (f) Z1000. Contour intervals are 0.5 m s^{-1} for U200 and 2 m for geopotential. Shaded areas exceed the 95% significance limit using *T* statistics.

6d,e,f) and observations (Figs. 6a,b,c). The latter are estimated from NCEP–NCAR and obtained by lagged regression onto the August–September SST SVD PC time series. The model develops a global quasi-barotropic response to the prescribed HS SST anomalies and reproduces fairly well the observed early winter atmospheric changes. The U200 zonally elongated tripole from the Tropics to high latitudes is well captured, especially on the eastern side of the basin. It corresponds to the reinforcement and eastward extension of the climatological subtropical upper-level jet. The Z500 stationary waves are accordingly modified. A clear barotropic negative NAO signal is extracted for NCEP–NCAR (Figs. 6b,c), and the Z1000 anomalies are very similar in location to the MSLP structure extracted by SVD (Fig. 1a). ARPEGE geopotential height responses (Figs. 6e,f) bear some resemblance to the observed patterns, with generally negative (positive) anomalies south (north) of 60°N. However, the strength and eastward extension of the positive anomalies near 60°–70°N are significantly underestimated in the model and the negative anomalies over the Barents Sea are opposite to observations.

A different picture emerges for the late summer (August–September) anomalies simulated by ARPEGE (Fig. 7). The Z500 NCEP–NCAR anomalies reveal a

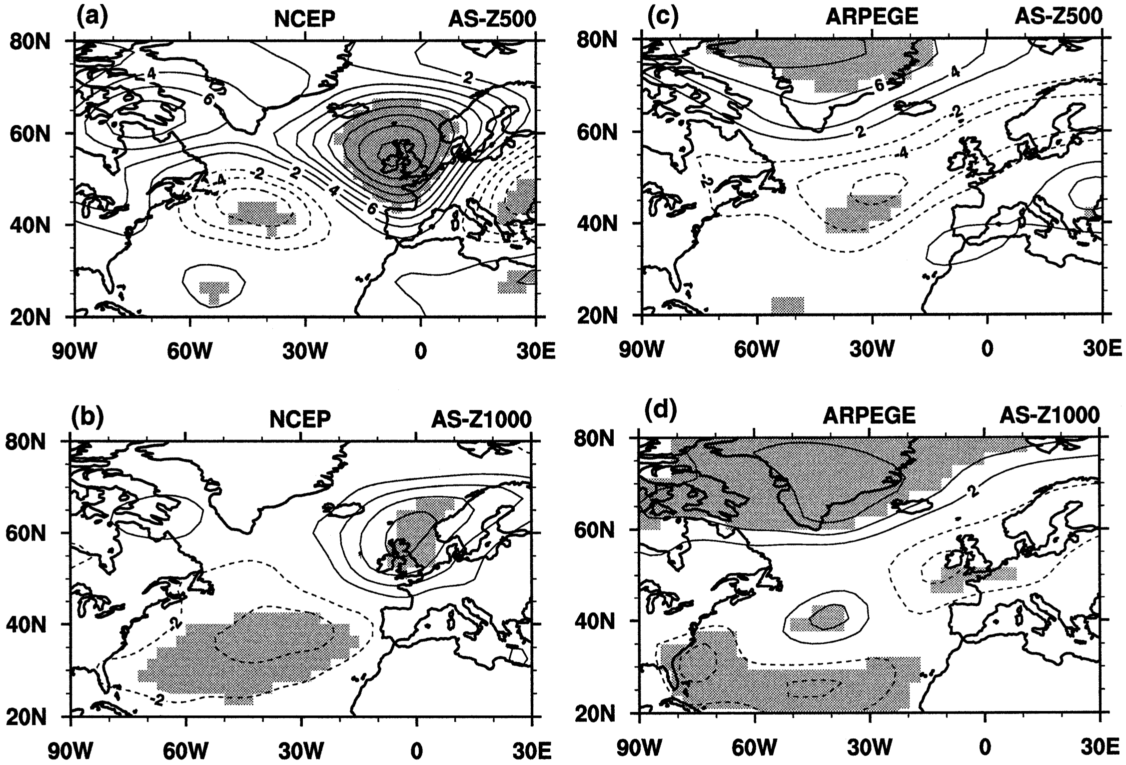

FIG. 7. As in Figs. 6b,c,d,f, but for the Aug–Sep mean.

clear wavy pattern emanating from the western tropical Atlantic basin and extending toward Scandinavia. This pattern bears a strong resemblance to the one obtained from the CCM3 sensitivity experiments as analyzed in the previous section for early summer. This result suggests that the tropical forcing of the midlatitude atmosphere is persistent over the entire season and therefore tends to reinforce the HS-type oceanic pattern initiated at the begining of summertime. ARPEGE results contrast strongly. The model does not capture the forced Rossby wave pattern at 500 hPa but departures between observed and modeled signals are even more striking in the lower troposphere. While a clear quasi-barotropic structure is extracted from NCEP–NCAR north of 35°N, the model develops a baroclinic response with high pressure anomalies at the surface over the cold waters off Newfoundland and low pressure anomalies off Ireland over warm SST conditions. The model's low-level response over the ocean is thus opposite to that from NCEP–NCAR. South of 30°N, both model and observation exhibit a baroclinic profile in agreement with the classical tropical/subtropical ocean–atmosphere relationship (Hoskins 1987). At higher latitudes (north of 65°N), the barotropic properties of the atmospheric flow are recovered in the model.

A couple of hypotheses may explain NCEP–NCAR/ARPEGE disagreements for late summer months at midlatitudes. The first one would refer to the nature of the experimental design, which could artificially perturb the low-level atmospheric response. It is well known that the so-called Atmospheric Model Intercomparison Project (AMIP) type simulations do not correctly capture the surface ocean–atmosphere interactions as developed in Barsugli and Battisti (1998) and may affect the barotropic shape of the atmospheric modes that dominates at midlatitudes. Such a mechanism might be seasonally dependant and could dominate in ARPEGE in summertime. A second hypothesis would be to consider the model as realistic and to assume that it correctly responds to the extratropical SST anomalies. The anomalous low-level circulation in the model then would tend to damp the surface ocean anomalies and would be consistent with the idea that the extratropical atmosphere is not responsible for the genesis of the extratropical anomalous HS lobes. Such a hypothesis reinforces the tropical origin of the anomalous extratropical atmospheric circulation suggested previously. It has been verified that no significant changes are simulated in ARPEGE within the tropical band. In particular, the Atlantic ITCZ is neither affected in intensity nor in position (not shown). In such a scenario, the switch between summer baroclinic and fall quasi-barotropic model response would also be considered as a realistic physical mechanism. The HS anomalies would then move from a *passive* role in summer to an *active* role in winter in the forcing of the extratropical atmosphere. In the rest of the paper, we further document such a hypothesis and focus our interest on the origin of the simulated baro-

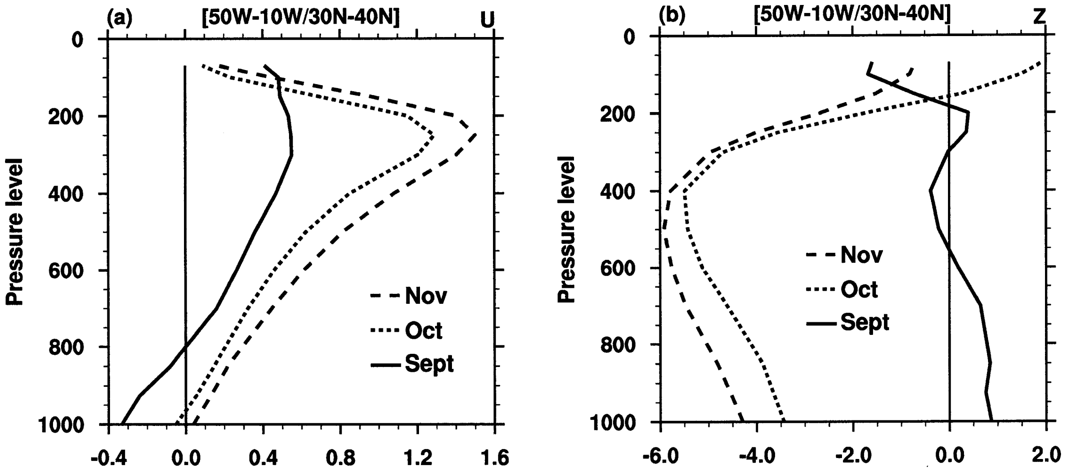

FIG. 8. Anomalous vertical profile for (a) zonal wind and (b) geopotential height for Sep–Nov months and averaged over the 30°–40°N, 50°–10°W domain. Units are respectively (m s^{-1}) and (m).

tropic response in fall. This will allow us to provide some possible explanations about the observed link between the phase of the summer oceanic HS mode and the early winter atmosphere.

c. Role of the climatological background in the simulated atmospheric response

Figure 8 shows anomalous vertical profiles of zonal wind and geopotential height in September, October, and November for the region (30°–40°N, 50°–10°W), which corresponds to the diffluence zone of the upper-tropospheric westerly wind jet and encompasses the maximum U200 westerly anomaly simulated by the model (Fig. 6d). While all three months exhibit positive vertical wind shear anomalies, the shear is amplified considerably in October and November compared to September (Fig. 8a). The vertical structure of the geopotential height response in the months with strong vertical wind shear is approximately equivalent barotropic whereas it is baroclinic in the months with weak shear (Fig. 8b). Why do similar SST anomaly patterns lead to different vertical structures of atmospheric circulation response in the presence of vertical wind shears?

Some studies suggest that anomalous transients and associated feedbacks onto the mean flow play an important role in shaping the midlatitude atmospheric response to extratropical SST anomalies (Held et al. 1989; Watanabe and Kimoto 1999). The relationship between synoptic-scale eddies along the midlatitude storm track and local vertical shear has been extensively documented in the literature (see, e.g., Hoskins and Valdez 1990). The model anomalous eddy activity estimated by the variance of the bandpass (2.2–6 days) filtered Z500 is presented in Fig. 9 as a function of latitude and for the same longitudinal band used in Fig. 8, for the months September, October, and November. The monthly U200 simulated anomalies are also shown. In September, although U200 westerly anomalies dominate significantly between 30° and 50°N, the storm activity (hereafter STA) is not significantly altered. In October however, westerly U200 anomalies between 30° and 45°N are accompanying by a significant enhancement in STA. In November, despite a slight 5° misfit, enhanced (reduced) STA coincides rather well in location over the entire eastern basin with U200 anomalous acceleration (slackening) and is overall amplified. Thus, it appears that increased vertical wind shear is accompanied by enhanced eddy activity changes from October onward suggesting, all together, a modification of the baroclinicity.

The alteration of the transients as well as their seasonality are presumably of central importance to explain the nature of the mean atmospheric response (Peng et al. 1995). Climatological monthly mean tendencies in U200 and STA computed as the difference between the given month and the previous one for the same region (30°–40°N, 50°–10°W) are shown in Fig. 9d. In September the mean STA is at its minimum amplitude, while the upper-level climatological jet already starts increasing over the selected area. It is hypothesized here that the baroclinic instability criteria are not met yet for September at this location. The jet might not be strong enough to trigger changes in storminess, despite locally enhanced vertical shear (Fig. 8a) interpreted as a direct response to the anomalous meridional temperature gradient imposed at the surface. From October onward U200 and STA are intensifying with maximum strengthening in November for the latter, one month later for the former. This crude analysis tends to indicate that the development of synoptic storms in the model requires a minimum speed of the jet. When such a threshold is overtaken, storms rapidly reach their maturity and do not follow as closely the gradual increase of the upper-level westerly circulation like in December. Due to a more favorable climatological background starting in

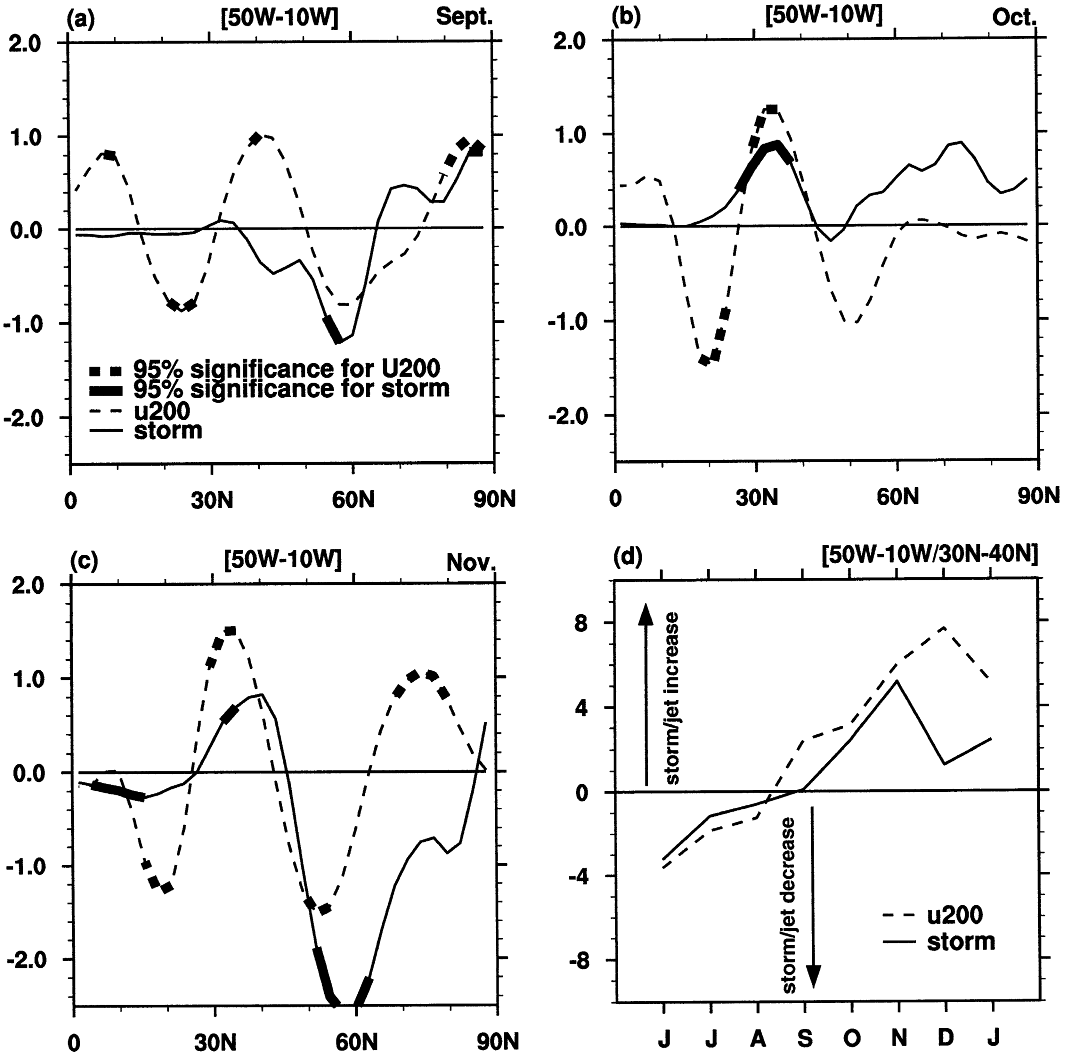

FIG. 9. Anomalous zonal wind at 200 hPa (U200) and storm track activity (STA) as a function of latitude and averaged over the longitudinal 40°–10°W band for (a) Sep, (b) Oct, and (c) Nov. Units are m s^{-1} and m^2. Thick superimposed lines exceed the 95% significance limit using *T* statistics. (d) Monthly changes for climatological U200 and STA, estimated as the difference between the mean value of the considered field for a given month and the one for a month earlier.

October, it is suspected, in our case, that the presence of local vertical shear, in relation to local prescribed SST anomalies, is now able to affect the local baroclinicity and related storminess at midlatitudes. It is thus suspected that the action of the storm explains to a great extent the barotropic nature of the mean atmospheric response from October. This hypothesis relies on the properties of the synoptic eddies to favor quasi-barotropic profiles as detailed, for instance, in Hoskins et al. (1983).

Beside its impact for explaining the nature of the atmospheric response, the alteration of the midlatitude STA may provide a strong positive feedback in maintaining and intensifying the modified mean flow. It is expected to affect the planetary-scale waves and to modify the stationary wave activity allowing for large-scale anomalous circulation. The latter clearly appears in November in the model as detailed below and is clearly amplified in December (not shown). The main storm track is significantly reduced over the entire North Atlantic from the Labrador Sea to the British Isles, while its southern edge is reinforced within a 30°–45°N latitudinal band (Fig. 10a). Such a pattern is consistent with the negative phase of the NAO as described in Hurrell (2003). The simulated pattern bears some resemblance with NCEP–NCAR changes estimated by November lagged regression of the bandpass-filtered Z500 on the AS SVD PC time series (Fig. 10c), especially east of 40°W. ARPEGE tends, however, to underestimate the alteration of the synoptic eddies on the western side of the basin (Newfoundland area) at midlatitudes and to overestimate the storminess reduction farther north.

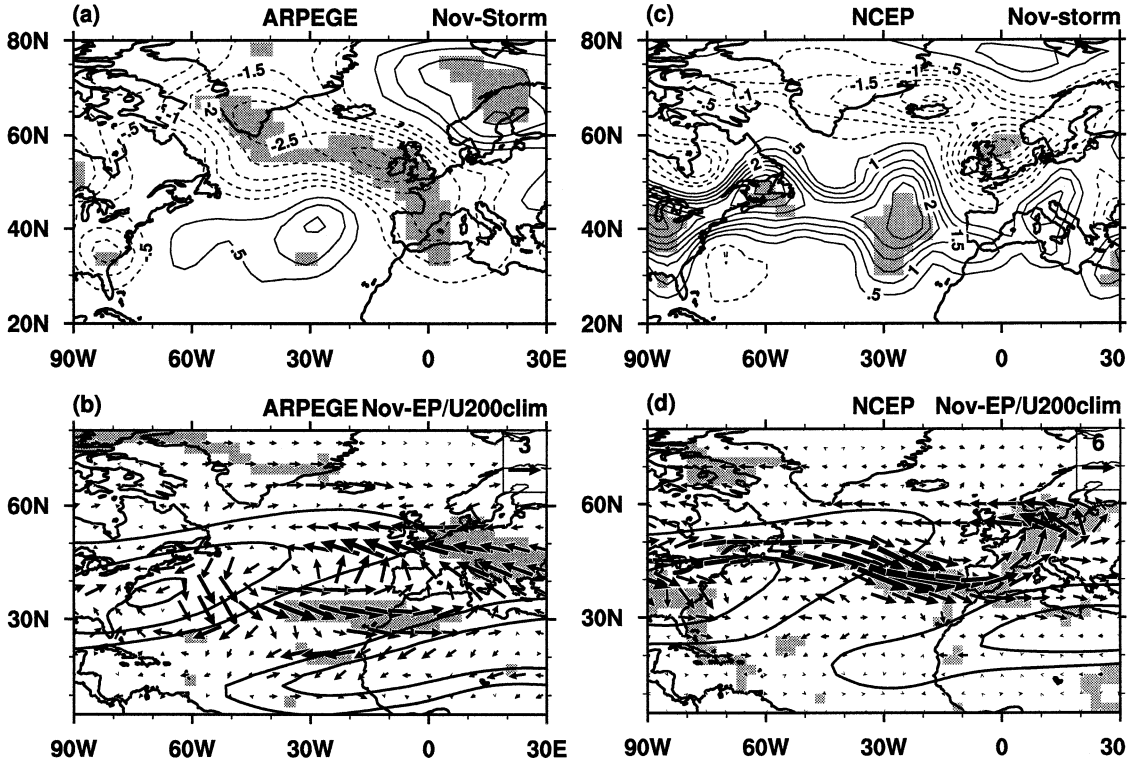

FIG. 10. Linear ARPEGE model response in Nov for the (a) STA (m^2) and (b) for the Eliassen–Palm (EP) flux. The mean model zonal wind at 200 hPa (U200) climatology is superimposed ($m\ s^{-1}$; thick solid line) and contours start at 20 $m\ s^{-1}$, every 10 $m\ s^{-1}$. Regression of NCEP–NCAR Nov (c) STA and (d) EP onto AS SST time series obtained from SVD. Contour intervals for STA are 0.5 m^2 and shaded areas exceed the 95% significance limit using *T* statistics. The mean NCEP–NCAR U200 (thick solid line) is superimposed (d).

Such a discrepancy can be attributed to the mean bias of the model (position and strength of the storm track and the jet) and the reader is invited to refer to Cassou and Terray (2001) or Drévillon et al. (2003) for further details.

Anomalous momentum fluxes associated with synoptic eddies are presented in Figs. 10b,d for the model and NCEP–NCAR observations using the Eliassen–Palm (EP) **E** vector following Trenberth's (1986) definition. The zonal **E** component can be interpreted as the zonal stretching of the mean flow induced by the synoptic eddies and its meridional component as the dominant eddy forcing of the mean streamfunction evolution (Held et al. 1989). The divergence (convergence) of **E** is indicative of mean flow acceleration (deceleration) due to the presence of STA changes. A clear divergence occurs in the model on the southeastern side of the mean climatological jet (around 30°N and within 40°–10°W) and is compensated by a strong convergence at its tail end off western Europe and at the entrance of the African subtropical jet. Such an anomaly is consistent with enhanced zonality of the basic flow and diminution of the planetary wave activity (Doblas-Reyes et al. 2001). It is also consistent with the forcing tendency due to synoptic eddies to develop a negative NAO-type large-scale pattern, as the strength of the Azores high (Icelandic low) is affected by the change in the main course of the storms. Despite a clear 10° displacement to the north that can be related again to the model mean bias, a similar pattern can be found in NCEP–NCAR. The EP divergence (convergence) is maximum along the southern (northern) edge of the mean jet over the eastern basin (east of 40°W).

4. Conclusions

a. Synthesis

Seasonal ocean–atmosphere interaction in the Atlantic has been investigated to obtain a better understanding of the statistical relationship between the summer SST anomalies associated with the ''Horseshoe'' mode and the NAO in the following early winter. A combined observational and modeling approach was adopted to examine the origin of the HS pattern and to provide some physical hypotheses for the delayed HS forcing on the next winter atmospheric circulation.

The results collectively suggest that HS can be primarily considered as an extratropical oceanic footprint of tropical convection changes in the Atlantic ITCZ via atmospheric teleconnection mechanisms. When the climatological ITCZ is enhanced or displaced northward, the atmospheric circulation is characterized by a cyclonic circulation off Newfoundland and diminished trade winds in the subtropics. The midlatitude atmospheric alteration is speculated to be the surface signature of forced Rossby waves initiated within the Tropics. This hypothesis is confirmed from model experiments using CCM3, where diabatic heating anomalies diagnosed from observations are imposed along the ITCZ. Anomalous convection in the western tropical basin is responsible in CCM3 for the excitation of a forced wave train extending northeastward from the Caribbian basin toward Scandinavia. Modifications in trade wind intensity in the northern tropical Atlantic occurs at the same time as a response to altered rainfall over the Sahel. The model teleconnection pattern reproduces fairly well the observed anomalous low-level atmospheric flow related to HS. The associated turbulent and radiative fluxes at the sea surface would tend to warm up the eastern and subtropical basins and cool the region east of Newfoundland, as observed. This allows us to conclude that the HS can be viewed as the local imprint of tropically induced extratropical atmospheric changes.

The late summer SST anomalies associated with the HS pattern were hypothesized to influence the atmospheric circulation over the North Atlantic and Europe in late fall/early winter. To test this observational hypothesis, experiments with ARPEGE were performed where the observed evolution of the HS mode is prescribed from August to November in the model SST boundary conditions. The model response is characterized by a baroclinic structure through September with high (low) surface pressure above cold (warm) SST anomalies, followed by an equivalent barotropic structure from October onward that resembles the NAO. The baroclinic response can be interpreted as the atmospheric tendency to damp the extratropical SST anomalies and may confirm the fact that the extratropical atmosphere by itself is not responsible for the HS. The barotropic response can be considered as the signature of large-scale atmospheric circulation in response to the extratropical SST anomalies. We have shown that anomalous vertical shear collocated with the anomalous meridional SST gradient is associated with changes in storm activity starting in October. The alteration of the storm track is hypothesized to be of central importance to initiate and sustain large-scale barotropic anomalies through eddy–mean flow interaction. The model seems to be more receptive to the SST anomalies when the storminess and associated upper-level jet are well developed. This emphasizes the importance of the climatological background to explain the sign and the timing of the atmospheric response to the persistent HS SST anomalies (see also Peng et al. 1995 but for late winter).

b. Discussion

The analyses presented here from observations and from model experiments have insisted on the importance of both summer tropical and extratropical conditions for possibly influencing the next winter's NAO. Tropical atmospheric changes seem to initiate a bridge between summer and early winter, and the resulting extratropical SST anomalies seems to be of importance as they persist enough to feed back to the atmosphere when the climatological background state is favorable. Therefore, it is important to consider together, in a global perspective, tropical and extratropical signals as they are not independent and contribute, by a cooperative and constructive interaction, to the variability of the winter NAO. It would be interesting, in particular, to test the ocean–atmosphere link presented in this paper from coupled model integrations.

In such a context, we can expand the present seasonal summer-to-winter bridge and propose a winter-to-winter bridge to explain the year-to-year persistence of the NAO and part of its low frequency. Let us now start with the winter–early spring season (from January to late April) and a given phase of the NAO. As described in the introduction, the prevailing forcing of the atmosphere on the underlying ocean during the winter–early spring months imprints a tripolelike structure of SST anomalies, which tends to be maximum in spring (Cayan 1992). Anomalous trade wind intensity peaks at that time (Hastenrath and Greischar 1993) and tends to build or reinforce the so-called oceanic interhemispheric SST gradient in the deep Tropics. As detailed in Sutton et al. (2000), the atmospheric response to the oceanic cross-equatorial gradient is maximum for late spring/summer months (June–September) and is characterized by a meridional displacement of the ITCZ toward the warmer hemisphere. We have now established a link between the summer tropical change and the *previous* winter NAO conditions. Vimont et al. (2001) have diagnosed a similar connection, but for the Pacific Ocean. Based on that link and on the present study on the relationship between summer SST conditions and the *next* winter's NAO, the same NAO phase as the previous winter would be favored and a new cycle would start with the reappearance of the same-sign winter North Atlantic SST tripole. Summer months might thus appear very important since, first, they are sensitive to the tropical SST anomalies forced to a great extent by the previous winter–spring NAO and, second, they prepare the extratropical oceanic HS anomalies to which the atmosphere is sensitive at the beginning of next winter. This temporal bridge over summer might explain part of the redenning of the winter NAO spectrum.

How can this bridge or cycle be interrupted? We have shown that the key vector sustaining the global mechanism is associated with the tropical convection over the western part of the Atlantic basin and over the Sahel to a lesser extent. A simple analysis of variance (ANOVA) shows that the internal atmospheric variability dominates in this region despite being located within the Tropics. It represents between 55% and 70% of the total variance depending on season, as estimated from

ARPEGE (Cassou and Terray 2001), and can therefore disrupt the bridge. In addition to this internal component, El Niño–Southern Oscillation is one obvious candidate to alter the Atlantic cycle as it remotely affects the strength and the position of the tropical convergence zones (Klein et al. 1999; Sutton et al. 2000; Giannini et al. 2001; Alexander et al. 2002). The local interaction between the land and the atmosphere over the South American continent might also play a role (Geldney and Valdez 2000), as well as the Indian Ocean variability via its effect on the branch of the Walker circulation over the African continent. The so-called ‘‘Atlantic Niño’’ (Zebiak 1993; Czaja and Frankignoul 2002) is also expected to modify the convection pattern of the tropical Atlantic and ultimately affects the midlatitudes (Drévillon et al. 2003).

Finally, the decadal variability of the subtropical and subpolar gyres (Sutton and Allen 1997) might modulate the efficiency of the remote tropical influences in imprinting extratropical SST anomalies, depending on the phase of the low frequency oceanic mode. Above all, we have to keep in mind that the internal dynamics of the extratropical North Atlantic atmosphere is by far dominant, even in summer, and can also create its own oceanic surface anomalies that may affect the following winter NAO. A large amount of variance of the total extratropical variability is controlled by internal atmospheric processes and the present study only explains about 15%–20% of the signal (based on the ARPEGE model response using ANOVA techniques, Cassou and Terray 2001).

Nevertheless, the lagged relationship between the summer SST anomalies and the following winter atmospheric circulation anomalies might be exploited for predictability purposes (Rodwell and Folland 2002). The scenario presented here, however, may be too limited due to the linear constraint on the analyses. Following a nonlinear approach used in Cassou et al. (2004) based on cluster analysis, it appears that the negative phase of the NAO is indeed preferably linked to the previous summer HS mode, whereas the positive phase of the NAO is better associated with a different summer SST structure more reminiscent of the SST tripole. It would therefore be interesting to further investigate the asymmetry between the positive and negative phase of the NAO and their relationship with previous oceanic conditions.

Acknowledgments. This work is supported by the European Community via the 5th framework program PREDICATE project under Contract EVK2-CT-1999-00020 and by NOAA under Grant NA06GP0394. The authors want to thank A. Giannini, R. Sutton, J. Chiang, and K. Trenberth for stimulating discussions. The first author is grateful to E. Maisonnave, S. Valcke, and C. Périgaud for their constant support and valuable critiques and to A. Phillips for help accessing and plotting the data with the NCL software.

REFERENCES

Alexander, M. A., I. Bladé, M. Newman, J. R. Lanzante, N. C. Lau, and J. D. Scott, 2002: The atmospheric bridge: The influence of ENSO teleconnections on air–sea interaction over the global oceans. *J. Climate,* **15,** 2205–2231.

Barsugli, J., and D. S. Battisti, 1998: The basic effects of atmosphere–ocean thermal coupling on midlatitude variability. *J. Atmos. Sci.,* **55,** 477–493.

Battisti, D. S., U. S. Bhatt, and M. A. Alexander, 1995: A modeling study of the interannual variability in the wintertime North Atlantic Ocean. *J. Climate,* **8,** 3067–3083.

Branstator, G., and S. E. Haupt, 1998: An empirical model of barotropic atmospheric dynamics and its response to tropical forcing. *J. Climate,* **11,** 2645–2667.

Cassou, C., and L. Terray, 2001: Oceanic forcing of the wintertime low-frequency atmospheric variability in the North Atlantic European sector: A study with the ARPEGE model. *J. Climate,* **14,** 4266–4291.

——, ——, J. W. Hurrell, and C. Deser, 2004: North Atlantic winter climate regimes: Spatial asymmetry, stationarity with time, and oceanic forcing. *J. Climate,* **17,** 1055–1068.

Cayan, D. R., 1992: Latent and sensible heat flux anomalies over the northern oceans: Driving the sea surface temperature. *J. Phys. Oceanogr.,* **22,** 859–881.

Czaja, A., and C. Frankignoul, 1999: Influence of the North Atlantic SST on the atmospheric circulation. *Geophys. Res. Lett.,* **26,** 2969–2972.

——, and ——, 2002: Observed impact of Atlantic SST anomalies on the North Atlantic Oscillation. *J. Climate,* **15,** 606–623.

de Coëtlogon, G., and C. Frankignoul, 2003: Persistence of winter sea surface temperature in the North Atlantic. *J. Climate,* **16,** 1364–1377.

Déqué, M., C. Dreveton, A. Braun, and D. Cariolle, 1994: The climate version of Arpege/IFS: A contribution to the French community climate modelling. *Climate Dyn.,* **10,** 249–266.

Deser, C., and M. S. Timlin, 1997: Atmosphere–ocean interaction on weekly timescales in the North Atlantic and North Pacific. *J. Climate,* **10,** 393–408.

——, M. A. Alexander, and M. S. Timlin, 2003: On the persistence of sea surface temperature anomalies in midlatitudes. *J. Climate,* **16,** 57–72.

Doblas-Reyes, F. J., M. Déqué, F. Valero, and D. B. Stephenson, 1998: North Atlantic wintertime intraseasonal variability and its sensitivity to GCM horizontal resolution. *Tellus,* **50A,** 573–595.

——, M. A. Pastor, M. J. Casado, and M. Déqué, 2001: Wintertime westward-travelling planetary scale perturbations over the Euro–Atlantic region. *Climate Dyn.,* **17,** 811–824.

Drévillon, M., L. Terray, P. Rogel, and C. Cassou, 2001: Midlatitude Atlantic SST influence on European winter climate variability in the NCEP–NCAR Reanalysis. *Climate Dyn.,* **18,** 331–344.

——, C. Cassou, and L. Terray, 2003: Model study of the wintertime atmospheric response to fall tropical Atlantic SST anomalies. *Quart. J. Roy. Meteor. Soc.,* **129,** 2591–2611.

Fontaine, B., S. Janicot, and P. Roucou, 1999: Coupled ocean–atmosphere surface variability and its climate impacts in the tropical Atlantic region. *Climate Dyn.,* **15,** 451–473.

Frankignoul, C., and K. Hasselmann, 1977: Stochastic climate models. Part II: Application to sea surface temperature variability and thermocline variability. *Tellus,* **29,** 284–305.

——, A. Czaja, and B. L’Hévéder, 1998: Air–sea feedback in the North Atlantic and surface boundary conditions for ocean models. *J. Climate,* **11,** 2310–2324.

Gedney, N., and P. J. Valdez, 2000: The effect of Amazonian deforestation of the Northern Hemisphere circulation and climate. *Geophys. Res. Lett.,* **27,** 3053–3056.

Giannini, A., M. A. Cane, and Y. Kushnir, 2001: Interdecadal changes in the ENSO teleconnection to the Caribbean region and the North Atlantic Oscillation. *J. Climate,* **14,** 2867–2879.

——, R. Saravanan, and P. Chang, 2003: Oceanic forcing of Sahel rainfall on interannual and interdecadal time scales. *Science,* **302,** 1027–1030.

Hastenrath, S., and L. Greischar, 1993: Circulation mechanisms related to northeast Brazil rainfall anomalies. *J. Geophys. Res.,* **98,** 5093–5102.

Held, I. M., S. W. Lyons, and S. Nigam, 1989: Transients and the extratropical response to El Niño. *J. Atmos. Sci.,* **46,** 163–174.

Hoerling, M. P., J. W. Hurrell, and T. Xu, 2001: Tropical origins for North Atlantic climate change. *Science,* **292,** 90–92.

Hoskins, B., 1987: Diagnostics of forced and free variability in the atmosphere. *Atmospheric and Oceanic Variability,* H. Cattle, Ed., Royal Meteorological Society, 57–74.

——, and R. Pierce, 1983: *Large Scale Dynamical Processes in the Atmosphere.* Academic Press, 397 pp.

——, and P. J. Valdez, 1990: On the existence of storm tracks. *J. Atmos. Sci.,* **47,** 1854–1864.

——, I. James, and G. White, 1983: The shape, propagation and mean flow interaction of large scale weather systems. *J. Atmos. Sci.,* **40,** 1595–1612.

Hulme, M., and M. G. New, 1997: Dependence of large-scale precipitation climatologies on temporal and spatial sampling. *J. Climate,* **10,** 1099–1113.

Hurrell, J. W., 2003: An overview of the North Atlantic Oscillation. *Geophys. Monogr. Series,* No. 134, Amer. Geophys. Union, 1–22.

——, J. J. Hack, B. A. Boville, D. L. Williamson, and J. T. Kiehl, 1998: The dynamical simulation of the NCAR Community Climate Model version 3 (CCM3). *J. Climate,* **11,** 1207–1236.

——, M. P. Hoerling, A. Phillips, and T. Xu, 2004: Twentieth century North Atlantic climate change. Part I: Assessing determinism. *Climate Dyn.,* in press.

Kalnay, E., and Coauthors, 1996: The NCEP/NCAR 40-Year Reanalysis Project. *Bull. Amer. Meteor. Soc.,* **77,** 437–471.

Kiehl, J. T., J. J. Hack, G. B. Bonan, B. A. Boville, B. P. Briegleb, D. L. Williamson, and P. J. Rasch, 1996: Description of the NCAR Community Climate Model (CCM3). NCAR Tech. Note NCAR TN-420+STR, 152 pp. [Available from NCAR, Boulder, CO 80307.]

Klein, S. A., B. J. Soden, and N. G. Lau, 1999: Remote sea surface temperature variations during ENSO: Evidence for a tropical atmospheric bridge. *J. Climate,* **12,** 917–932.

Kushnir, Y., W. A. Robinson, I. Bladé, N. M. J. Hall, S. Peng, and R. T. Sutton, 2002: Atmospheric GCM response to extratropical SST anomalies: Synthesis and evaluation. *J. Climate,* **15,** 2233–2256.

Marshall, J., and Coauthors, 2001: Review: North Atlantic climate variability: Phenomena, impacts and mechanisms. *Int. J. Climatol.,* **21,** 1863–1898.

Mehta, V. M., M. J. Suarez, J. V. Manganello, and T. Delworth, 2000: Oceanic influence on the North Atlantic Oscillation and associated Northern Hemisphere climate variations, 1959–1993. *Geophys. Res. Lett.,* **27,** 121–124.

Norris, J. R., Y. Zhuang, and J. W. Wallace, 1998: Role of low clouds in summertime atmosphere–ocean interactions over the North Pacific. *J. Climate,* **11,** 2482–2490.

Okumura, Y., S. P. Xie, A. Numaguti, and Y. Tanimoto, 2001: Tropical Atlantic air–sea interaction and its influence on the NAO. *Geophys. Res. Lett.,* **28,** 1507–1510.

Peng, S., and J. S. Whitaker, 1999: Mechanisms determining the atmospheric response to midlatitude SST anomalies. *J. Climate,* **12,** 1393–1408.

——, and W. A. Robinson, 2001: Relationships between atmospheric internal variability and the responses to an extratropical SST anomaly. *J. Climate,* **14,** 2943–2959.

——, L. A. Mysak, H. Ritchie, J. Derome, and B. Dugas, 1995: The difference between early and midwinter atmospheric responses to sea surface temperature anomalies in the northwest Atlantic. *J. Climate,* **8,** 137–157.

——, W. A. Robinson, and S. Li, 2003: Mechanisms for the NAO responses to the North Atlantic SST tripole. *J. Climate,* **16,** 1987–2004.

Robinson, W. A., 2000: Review of WETS—The workshop on extratropical SST anomalies. *Bull. Amer. Meteor. Soc.,* **81,** 567–577.

Rodwell, M. J., and C. K. Folland, 2002: Atlantic air–sea interaction and seasonal predictability. *Quart. J. Roy. Meteor. Soc.,* **128,** 1413–1443.

——, D. P. Rowell, and C. K. Folland, 1999: Oceanic forcing of the wintertime North Atlantic Oscillation and European climate. *Nature,* **398,** 320–323.

Sardeshmukh, P. D., and B. J. Hoskins, 1988: The generation of global rotational flow by steady idealized tropical divergence. *J. Atmos. Sci.,* **45,** 1228–1251.

Stephenson, D. B., H. Wanner, S. Brønnimann, and J. Luterbacher, 2003: The history of scientific research on the North Atlantic Oscillation. *Geophys. Monogr.,* No. 134, Amer. Geophys. Union, 37–50.

Sutton, R. T., and M. R. Allen, 1997: Decadal variability of North Atlantic sea surface temperature and climate. *Nature,* **388,** 563–567.

——, and D. L. R. Hodson, 2003: The influence of the ocean on North Atlantic climate variability 1871–1999. *J. Climate,* **16,** 3269–3313.

——, S. P. Jewson, and D. P. Rowell, 2000: The elements of climate variability in the tropical Atlantic region. *J. Climate,* **13,** 3261–3284.

——, W. A. Norton, and S. P. Jewson, 2001: The North Atlantic Oscillation—What role for the ocean? *Atmos. Sci. Lett.,* **1,** 89–100.

Terray, L., and C. Cassou, 2002: Tropical Atlantic sea surface temperature forcing of the quasi-decadal climate variability over the North Atlantic–Europe region. *J. Climate,* **15,** 3170–3187.

Trenberth, K. E., 1986: An assessment of the impact of transient eddies on the zonal flow during a blocking episode using localized Eliassen–Palm flux diagnostics. *J. Atmos. Sci.,* **43,** 2070–2087.

Vimont, D. J., D. S. Battisti, and A. C. Hirst, 2001: Footprinting: A seasonal link between the midlatitudes and tropics. *Geophys. Res. Lett.,* **28,** 3923–3926.

Wallace, J. M., and D. Gutzler, 1981: Teleconnections in the geopotentiel fields during the Northern Hemisphere winter. *Mon. Wea. Rev.,* **109,** 784–812.

Watanabe, M., and M. Kimoto, 1999: Tropical–extratropical connection in the Atlantic atmosphere ocean variability. *Geophys. Res. Lett.,* **26,** 2247–2250.

——, and ——, 2000: Atmosphere–ocean thermal coupling in the North Atlantic: A positive feedback. *Quart. J. Roy. Meteor. Soc.,* **126,** 3343–3369.

Webster, P. J., 1982: Seasonality in the local and remote atmospheric response to sea surface temperature anomalies. *J. Atmos. Sci.,* **39,** 722–733.

Woodruff, S. D., H. F. Diaz, J. D. Elms, and S. J. Worley, 1998: COADS Release 2 data and metadata enhancements for improvements of marine surface flux fields. *Phys. Chem. Earth,* **23,** 517–527.

Zebiak, S., 1993: Air–sea interaction in the equatorial Atlantic region. *J. Climate,* **6,** 1567–1586.